JOURNAL OF AIRCRAFT
Vol. 35, No. 2, March–April 1998

Stability of a Towed Body

Bernard Etkin*
University of Toronto, Toronto, Ontario M3H 5T6, Canada

This paper presents a mathematical model for the efficient computation of the stability of bodies subject to fluid–dynamic forces while constrained by a flexible, extensible cable. The way the cable is represented permits the body to be heavier or lighter than air and to have a steady-state lift. The model is applied to the case of a pendant vehicle towed by a cable attached to an aircraft, a case of considerable practical interest. It is shown that inherent instabilities are present and that they can be eliminated by the correct method of cable attachment. The paper emphasizes the physics of the system and the reasons for the instabilities.

Nomenclature

a, b, b'	= dimensions, Fig. 3
d	= diameter of cable
E	= Young's modulus
F_B	= body-fixed frame of reference
F_I	= inertial frame of reference, moving horizontally with speed V_0
g	= gravitational acceleration
h	= length of cable segment
I_x, I_y, I_z	= moments of inertia, body axes
L, D	= lift and drag per unit length of cable, also lift and drag of the towed body
l	= length of cable
m	= mass of body
N	= number of points on cable
p, q, r	= angular velocity components of the body
s	= curvilinear coordinate on cable
T	= tension in cable
T_{Ny}	= y_B component of cable tension at point N
u, v, w	= velocity components of cable point relative to F_I
u', v', w'	= perturbation velocity components in F_B of the body c.g., relative to atmosphere
u_Q, v_Q, w_Q	= F_B components of velocity of point Q
V_0	= steady flight speed
W	= weight of towed body
X, Y, Z	= aerodynamic force per unit length of cable in frame F_I, also aerodynamic force on towed body in frame F_B
x, y, z	= coordinates of a point on the cable, in frame F_I
α	= angle attack of the body
α_c	= angle, Fig. 2
γ	= angle, Fig. 2
δ	= static extension of elastic cable
δ_c	= angle, Fig. 2
θ, ϕ, ψ	= Euler angles of towed body
ξ, η, ζ	= perturbations of x, y, z
ρ_c	= mass per unit length of cable
ϕ	= angle, Fig. 3a

Superscripts

$\bar{}$	= steady-state value
$'$	= perturbation value

Received June 23, 1997, revision received Oct. 4, 1997; accepted for publication on Oct. 19, 1997.

*Professor Emeritus, Institute for Aerospace Studies, 4925 Dufferin Street, North York.

I. Introduction

THERE are numerous physical systems in which a body is acted on by fluid–dynamic forces while being constrained by a cable. Examples include kites, towed gliders, tethered aerostats, towed sonar devices, trailing static-pressure devices, refueling hoses, and the vehicles used to carry geophysical instrumentation beneath an aircraft. It is the last application that provided the motivation for this work.

As everyone who has flown a kite knows, stability can be a problem in such systems. An inherently stable aerodynamic body can become unstable when its propulsion, so to speak, is provided by a cable instead of an aerodynamic thruster. Bodies on which the only aerodynamic force is drag will never be unstable. On the other hand, when the body is configured so as to maintain its attitude when in motion, as, for example, with tail fins, then lift and side-force can be present. Couplings can then occur between body attitude degrees of freedom and cable degrees of freedom, which can lead to instability of small perturbations. As pointed out by DeLaurier,[1] the consequence of such an instability may be a stable limit cycle of finite amplitude. There are numerous anecdotal reports of finned bodies experiencing unacceptably large motions, both longitudinal and lateral. Because such oscillations of the towed body are unlikely to be acceptable from an operational standpoint, stability of small perturbations may be taken to be a requirement in the design of such systems.

The earliest research on this phenomenon appears to be that carried out in England during WWI by Bairstow et al.,[2] and subsequently by Glauert,[3] as well as by others. Glauert used a very simple model, a massless, dragless inextensible wire towing an aerodynamically stable body, to demonstrate the possibility of system instability. Later work in England (see Ref. 4) extended the sophistication of the analysis by including some consideration of the cable's physical characteristics. Etkin and Mackworth[5] used an analysis similar to that of Glauert and carried out wind-tunnel experiments with a finned body that verified the theory. DeLaurier[1] presented the first modern analysis with a comprehensive model of a cable-body system having an inextensible cable. His analysis recognized that the cable can be truly represented only by a partial differential equation, with the attached body providing end conditions. In all of these studies the tow point was either stationary or had constant velocity. This constraint was released by de Matteis,[4] who studied the longitudinal stability of a system comprising a tow plane, an extensible cable, and a towed glider. This system was shown to have possible important instabilities involving the tow plane. The modeling of these systems, with a realistic representation of the cable included, inevitably leads to a complex mathematical problem, and a variety of detailed formulations have been used. All require

machine computation to obtain solutions. The formulation presented herein brings the problem into the domain of conventional linear analysis, leading to a generalized eigenvalue problem that is readily computed by available commercial software.

To obtain a reliable and sufficiently general model to cover a range of practical cases, it is necessary to include all of the previously mentioned properties of the cable, i.e., aerodynamic force, inertia, and extensibility. For further generality we have also included an approximation to internal damping. This takes the form of linear viscous energy dissipation, which, although not an accurate representation of real hysteretic processes, is adequate for the present purpose. The one significant approximation that remains is that the cable has no bending stiffness. This assumption is reasonable for many practical cases.

Here we begin the analysis with the exact differential equations of a flexible extensible cable, and use a finite difference representation of the s derivatives to generate a system of ordinary differential equations in t. This makes it possible to use a compact representation of the equations in matrix form and to solve them very conveniently. The particular form of the equations and the representations of the aerodynamic forces and the geometry were carefully chosen so as to make the analysis and the final structure of the system as transparent and as simple as possible. The equations describing the cable are quite general and are indeed applicable to all of the many situations described in the preceding text. However, for each case it is necessary to specialize the equations describing the towed body and the motion of the tow point to correspond to the physical configuration under study. In the examples computed next, we have specialized to a pendant body, i.e., a nonbuoyant body with a small ratio of lift-to-weight. The tow point is assumed to move at constant horizontal speed. We have chosen a cylindrical body with a rounded nose and cruciform fins for the primary example. To validate the model, we have also applied it to the limiting cases of a simple pendulum, a compound pendulum, and a dangling cable with no body attached.

The computed results show that this class of system can have inherent instabilities over some ranges of flight speed. This confirms the finding in Refs. 2 and 5 for lateral stability of a much simplified model. We have also found, however, that the instability can be eliminated by a suitable method of attachment of the cable to the body.

II. Analysis

It is assumed that the system has a steady state at speed V_0 in still air. In the steady state the cable lies in a vertical plane that bisects a symmetrical body. It is the stability of this steady state that is to be studied.

Figure 1 shows that the coordinate system used (x_I, y_I, z_I) is an inertial frame F_I attached to the tow plane at O. It moves to the left with the constant horizontal velocity V_0; (x_B, y_B, z_B) is a noninertial body-fixed frame F_B attached to the body with origin at its c.g. and moving with it. The body axes are the principal axes of the body. The cable OP_N is attached to the tow plane at O and to the body sling at P_N. s is distance along the cable measured from O. N points P_N, equidistant in s in the steady state, are chosen on the cable. The coordinates in frame F_I of point P_n on the cable are (x_n, y_n, z_n).

It can be shown (the proof is not given here) that when the system is symmetrical about the xz plane, as this one is, then the most general motion (in still air) can, just as with airplanes, be subdivided into two classes, longitudinal and lateral. In the former, each particle of the cable and body moves in a vertical plane (parallel to xz), so that the motion of the body consists of surging (fore and aft), heaving (up and down), and pitching. In the latter class, the motion of the body consists of rolling, yawing, and sideslipping. Although the longitudinal class can exist by itself for both large and infinitesimal motions, the lateral class exists independently only for small perturbations.

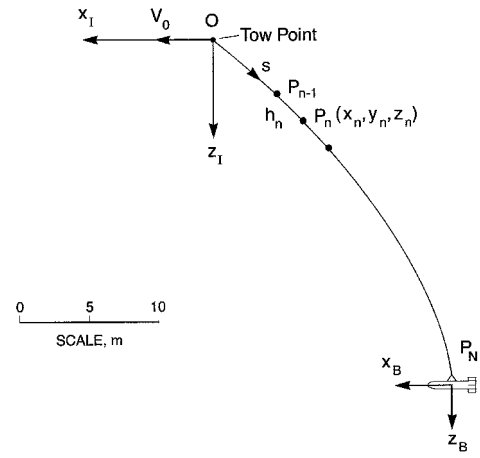

Fig. 1 Coordinate systems and steady state; example body at 60 m/s.

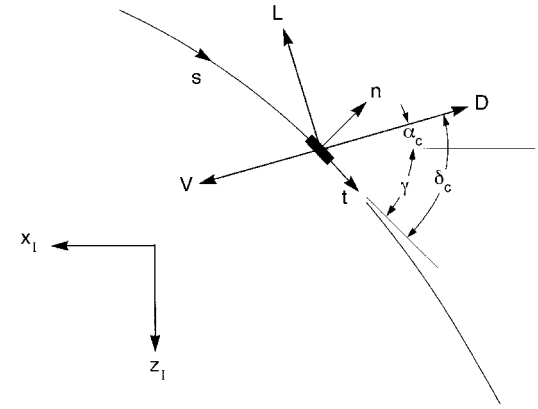

Fig. 2 Cable element in xz plane.

If the lateral motions are large, then they induce motions in the longitudinal degrees of freedom as well.

III. Longitudinal Model

A. Cable

An element of the cable of mass dm and length ds is shown with the relevant notation in Fig. 2. $\boldsymbol{t}$ and $\boldsymbol{n}$ are unit vectors tangent and normal to the cable centerline, and the x_I and z_I axes are horizontal and vertical, respectively. We denote the aerodynamic and gravity force vectors on the element by $\boldsymbol{A}$ ds and $\boldsymbol{G}$ ds, respectively, and the acceleration by $\boldsymbol{a}$. The components of the vectors in frame F_I are

$$\boldsymbol{t} = \begin{bmatrix} -\cos\gamma \\ 0 \\ \sin\gamma \end{bmatrix}, \qquad \boldsymbol{n} = \begin{bmatrix} -\sin\gamma \\ 0 \\ -\cos\gamma \end{bmatrix} \tag{1}$$

$$\boldsymbol{A} = \begin{bmatrix} X \\ 0 \\ Z \end{bmatrix}, \qquad \boldsymbol{G} = \begin{bmatrix} 0 \\ 0 \\ \rho_c g \end{bmatrix}, \qquad \boldsymbol{a} = \begin{bmatrix} \dot{u} \\ 0 \\ \dot{w} \end{bmatrix} \tag{2}$$

The net force applied to dm by the tension acting at its two ends is

$$\frac{\partial}{\partial s}(T\boldsymbol{t})\,\mathrm{d}s \tag{3}$$

The equation of motion is then

$$\boldsymbol{a}\,\mathrm{d}m = \boldsymbol{A}\,\mathrm{d}s + \boldsymbol{G}\,\mathrm{d}s + \frac{\partial}{\partial s}(T\boldsymbol{t})\,\mathrm{d}s \tag{4}$$

Table 1 Cable derivatives

	$k_1 = 1.1$	
	X	Z
u	$-\rho V_0 d\bar{C}_d$	$-\rho V_0 d\bar{C}_l$
w	$\frac{1}{2}\rho V_0 d(\bar{C}_l - 3k_1 \sin^2\bar{\gamma}\cos\bar{\gamma})$	$-\frac{1}{2}\rho V_0 d[k_1(2\sin\bar{\gamma}\cos^2\bar{\gamma} - \sin^3\bar{\gamma}) + \bar{C}_d]$
γ	$-\frac{3}{2}\rho V_0^2 d k_1 \sin^2\bar{\gamma}\cos\bar{\gamma}$	$-\frac{1}{2}\rho V_0^2 d k_1(2\sin\bar{\gamma}\cos^2\bar{\gamma} - \sin^3\bar{\gamma})$

The four equations that apply at any point of the cable are then the x and z components of Eq. (4) and two kinematic relations, i.e.,

$$\dot{x} = u, \qquad \dot{z} = w \tag{5}$$

$$\rho_c \dot{u} = X - \frac{\partial}{\partial s}(T\cos\gamma), \qquad \rho_c \dot{w} = Z + \rho_c g + \frac{\partial}{\partial s}(T\sin\gamma) \tag{6}$$

The perturbation equations are found to be

$$\dot{\xi} = u, \qquad \dot{\zeta} = w \tag{7a}$$

$$\rho_c \dot{u} = X' + \sin\bar{\gamma}\frac{d\bar{T}}{ds}\gamma' - \cos\bar{\gamma}\frac{dT'}{ds} + \sin\bar{\gamma}\frac{d\bar{\gamma}}{ds}T' + \bar{T}\cos\bar{\gamma}\frac{d\bar{\gamma}}{ds}\gamma' + \bar{T}\sin\bar{\gamma}\frac{d\gamma'}{ds} \tag{7b}$$

$$\rho_c \dot{w} = Z' + \cos\bar{\gamma}\frac{d\bar{T}}{ds}\gamma' + \sin\bar{\gamma}\frac{dT'}{ds} + \cos\bar{\gamma}\frac{d\bar{\gamma}}{ds}T' - \bar{T}\sin\bar{\gamma}\frac{d\bar{\gamma}}{ds}\gamma' + \bar{T}\cos\bar{\gamma}\frac{d\gamma'}{ds} \tag{7c}$$

1. Aerodynamic Forces on the Cable

The lift and drag per unit length of cable are shown in Fig. 2, together with the local velocity vector of the cable, and the angles α_c, γ, and δ_c

$$L = C_l \tfrac{1}{2}\rho V^2 d, \qquad D = C_d \tfrac{1}{2}\rho V^2 d \tag{8}$$

$$\delta_c = \alpha_c + \gamma \tag{9}$$

The lift and drag coefficients are based on data of Ref. 6. (This very old data has been used in most of the prior literature on this topic. It would make a good thesis project for a graduate student to make a new set of measurements.)

$$C_l = 1.1\sin^2\delta_c\cos\delta_c, \qquad C_d = 0.02 + 1.1\sin^3\delta_c \tag{10}$$

The aerodynamic forces in the x_I and z_I directions per unit length of cable are

$$X = -D\cos\alpha_c + L\sin\alpha_c, \qquad Z = -L\cos\alpha_c - D\sin\alpha_c \tag{11}$$

We have that

$$V^2 = (V_0 + u)^2 + w^2 \tag{12}$$

$$\alpha_c = \tan^{-1}[w/(V_0 + u)] \tag{13}$$

The perturbations in the X and Z forces at point n are given by

$$X' = \frac{\partial X}{\partial u}u + \frac{\partial X}{\partial w}w + \frac{\partial X}{\partial \gamma}\gamma', \qquad Z' = \frac{\partial Z}{\partial u}u + \frac{\partial Z}{\partial w}w + \frac{\partial Z}{\partial \gamma}\gamma' \tag{14}$$

From Eqs. (8) to (13) we get the matrix of aerodynamic derivatives of the cable to be as shown in Table 1. Each entry is the partial derivative of the column head with respect to the row variable.

2. Length Condition

It is assumed that each element of the cable is short enough to be treated as straight and, consequently, of length h_n obtained from

$$h_n^2 = (x_n - x_{n-1})^2 + (z_n - z_{n-1})^2 \tag{15}$$

The perturbation of Eq. (15) is

$$\bar{h}_n h_n' = (\bar{x}_n - \bar{x}_{n-1})\xi_n - (\bar{x}_n - \bar{x}_{n-1})\xi_{n-1} + (\bar{z}_n - \bar{z}_{n-1})\zeta_n - (\bar{z}_n - \bar{z}_{n-1})\zeta_{n-1} \tag{16}$$

When the cable is elastic, with viscous internal damping, the relation between the length and average tension is

$$\tfrac{1}{2}(T_n' + T_{n-1}') = c_1 h_n' + c_2 \dot{h}_n' \tag{17}$$

For a wire of cross-sectional area A and Young's modulus E, the constant c_1 is

$$c_1 = AE/\bar{h} \tag{18}$$

The constant c_2 can be related to energy dissipation. If ε is the fraction of maximum strain energy in a cable segment that is dissipated per cycle, it can be shown that

$$\varepsilon = \frac{2\pi\omega c_2}{\sqrt{c_1^2 + \omega^2 c_2^2}}$$

or approximately, for low frequency, which is the present case

$$c_2 = (\varepsilon/4\pi^2 f)c_1 \tag{19}$$

c_2 can thus be chosen to provide a selected energy dissipation at a selected frequency.

3. Geometry and the Finite Differences

We also require certain geometrical relations, as follows:

$$\frac{dz}{ds} = \sin\gamma, \qquad \frac{dx}{ds} = -\cos\gamma, \qquad \frac{d\zeta}{ds} = (\cos\bar{\gamma})\gamma', \qquad \frac{d\zeta}{ds} = (\sin\bar{\gamma})\gamma' \tag{20}$$

From Eq. (20) we can write γ' as a function of the cable displacement

$$\gamma' = \frac{1}{\sin\bar{\gamma}}\frac{d\xi}{ds} \tag{21}$$

and in the finite difference scheme

$$\left.\frac{d\xi}{ds}\right|_n = \frac{\xi_{n+1} - \xi_{n-1}}{2\bar{h}} \tag{22}$$

From Eq. (20) we get

$$\frac{d^2x}{ds^2} = \sin\gamma\frac{d\gamma}{ds} \tag{23}$$

The perturbation of Eq. (23) is

$$\frac{d^2\xi}{ds^2} = \sin\bar{\gamma}\frac{d\gamma'}{ds} + \frac{d\bar{\gamma}}{ds}\cos\bar{\gamma}\gamma'$$

from which we get

$$\frac{d\gamma'}{ds} = \frac{1}{\sin\bar{\gamma}}\frac{d^2\xi}{ds^2} - \cot\bar{\gamma}\frac{d\bar{\gamma}}{ds}\gamma' \tag{24}$$

The finite difference representation of the second derivative in Eq. (24) is

$$\left.\frac{d^2\xi}{ds^2}\right|_n = \frac{\xi_{n-1} - 2\xi_n + \xi_{n+1}}{\bar{h}^2} \tag{25}$$

When implementing the finite difference scheme at the endpoints of the cable, there are some expressions that require values of quantities that are not in the set of variables, e.g., ξ_{-1} in Eq. (25) for $n = 0$. For these instances, we use either a constant second difference, such as

$$\left.\frac{d^2\xi}{ds^2}\right|_n = \left.\frac{d^2\xi}{ds^2}\right|_{n-1}$$

or a one-sided difference such as [see Eq. (22)]

$$\left.\frac{d\xi}{ds}\right|_N = \frac{\xi_N - \xi_{N-1}}{\bar{h}}$$

The error introduced by finite differences diminishes with increasing N, which should therefore be increased until an acceptable limit is achieved.

B. Towed Body

The perturbation model for the body is obtained from Ref. 7, Eq. (4.9, 18), by modifying it to apply to principal body axes and by adding the effects of the cable tension T_N acting at P_N. It should be noted that u' and w' are components of the velocity of the c.g. relative to the stationary atmosphere. T_N is tangent to the cable at P_N and its components in F_B are

$$T_x = (\bar{T}_N + T'_N)\cos\phi, \qquad T_z = -(\bar{T}_N + T'_N)\sin\phi \tag{26}$$

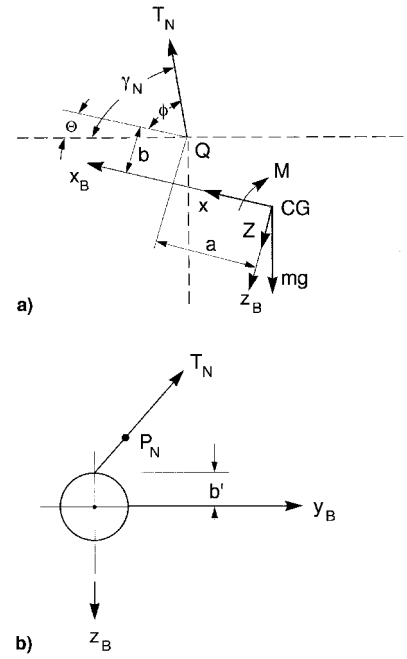

Fig. 3 Cable tension at the body.

Figure 3 shows the offsets a and b of the attachment point P_N and that $\phi = \gamma_N - \theta$. The perturbations in the tension components are then as in Eq. (27), and the differential equations for the body, written in terms of the perturbations of the body state variables, are given in matrix form in Eq. (28):

$$\begin{bmatrix} T'_x \\ T'_z \end{bmatrix} = \begin{bmatrix} -\bar{T}_N\sin\bar{\phi} & \bar{T}_N\sin\bar{\phi} & \cos\bar{\phi} \\ -\bar{T}_N\cos\bar{\phi} & \bar{T}_N\cos\bar{\phi} & \sin\bar{\phi} \end{bmatrix} \begin{bmatrix} \gamma'_N \\ \theta' \\ T'_N \end{bmatrix} \tag{27}$$

$$\begin{bmatrix} m\dot{u}' \\ m\dot{w}' \\ I_y\dot{q}' \\ \dot{\theta}' \end{bmatrix} = \boldsymbol{A}\begin{bmatrix} u' \\ w' \\ q' \\ \theta' \end{bmatrix} + \begin{bmatrix} 1 & 0 \\ 0 & 1 \\ -b & -a \\ 0 & 0 \end{bmatrix}\begin{bmatrix} T'_x \\ T'_z \end{bmatrix} \tag{28}$$

When Eq. (27) is substituted into Eq. (28), we get Eq. (29):

$$\begin{bmatrix} m\dot{u}' \\ m\dot{w}' \\ I_y\dot{q}' \\ \dot{\theta}' \end{bmatrix} = \boldsymbol{A}\begin{bmatrix} u' \\ w' \\ q' \\ \theta' \end{bmatrix} + \boldsymbol{B}\begin{bmatrix} \gamma'_N \\ \theta' \\ T'_N \end{bmatrix} \tag{29}$$

The matrices $\boldsymbol{A}$ and $\boldsymbol{B}$ are given by Eqs. (30) and (31), respectively. The $\dot{w}$ derivatives present in Ref. 7 have been neglected for the wingless body

$$\boldsymbol{A} = \begin{bmatrix} X_u & X_w & (X_q - mV_0\sin\bar{\theta}) & -mg\cos\bar{\theta} \\ Z_u & Z_w & (Z_q + mV_0\cos\bar{\theta}) & -mg\sin\bar{\theta} \\ M_u & M_w & M_q & 0 \\ 0 & 0 & 1 & 0 \end{bmatrix} \tag{30}$$

$$\boldsymbol{B} = \begin{bmatrix} -\bar{T}_N\sin\bar{\phi} & \bar{T}_N\sin\bar{\phi} & \cos\bar{\phi} \\ -\bar{T}_N\cos\bar{\phi} & \bar{T}_N\cos\bar{\phi} & -\sin\bar{\Phi} \\ (b\bar{T}_N\sin\bar{\phi} + a\bar{T}_N\cos\bar{\phi}) & -(b\bar{T}_N\sin\bar{\phi} + a\bar{T}_N\cos\bar{\phi}) & -(b\cos\bar{\phi} - a\sin\bar{\phi}) \\ 0 & 0 & 0 \end{bmatrix} \tag{31}$$

C. End Conditions

At the upper end of the cable, we have

$$\bar{x}_0 = \bar{z}_0 = \xi_0 = \zeta_0 = u_0 = w_0 = 0 \tag{32}$$

and at the match point P_N, the velocity relative to atmosphere must be the same whether calculated as a point of the cable or as a point of the towed body. That is

$$\begin{bmatrix} V_0 + u_N \\ w_N \end{bmatrix} = \begin{bmatrix} u_Q \cos\theta + w_Q \sin\theta \\ -u_Q \sin\theta + w_Q \cos\theta \end{bmatrix} \tag{33}$$

After taking the small perturbation of Eq. (33) we obtain the following match conditions:

$$\begin{aligned} u_N &= u' \cos\bar{\theta} + w' \sin\bar{\theta} - q'(a \sin\bar{\theta} + b \cos\bar{\theta}) \\ w_N &= -u' \sin\bar{\theta} + w' \cos\bar{\theta} + q'(b \sin\bar{\theta} - a \cos\bar{\theta}) \\ &\quad - V_0\theta' \end{aligned} \tag{34}$$

D. Steady State

The steady-state values of θ, x, z, T, and γ are all needed for the dynamic calculation. The first step in obtaining that solution is to calculate $\bar{\theta}$, the steady-state pitch attitude of the body. Let the basic aerodynamics of the body be given by

$$C_x(\alpha), \qquad C_z(\alpha), \qquad C_m(\alpha)$$

in which C_m is with respect to the c.g. Then at any speed V_0, setting the pitching moment about the attachment point to zero yields the following equation:

$$f(\alpha) = M(\alpha) + mg(a \cos\alpha - b \sin\alpha) + bX(\alpha) + aZ(\alpha) = 0 \tag{35}$$

Equation (35) is solved iteratively for $\alpha = \bar{\theta}$. Equilibrium of the forces on the body gives

$$\begin{aligned} \bar{T}_x &= -\bar{X} + mg \sin\bar{\theta}, \qquad \bar{T}_N = \sqrt{\bar{T}_x^2 + \bar{T}_z^2} \\ \bar{T}_z &= -\bar{Z} - mg \cos\bar{\theta}, \qquad \bar{\gamma}_N = \tan^{-1}[-(\bar{T}_z/\bar{T}_x)] + \bar{\theta} \end{aligned} \tag{36}$$

The next step is to integrate the cable equations numerically, beginning at P_N and proceeding toward the tow point. The four equations needed are from Eqs. (6) and (20)

$$\begin{aligned} \frac{\mathrm{d}}{\mathrm{d}s}(\bar{T}\cos\bar{\gamma}) &= \bar{X}, \qquad \frac{\mathrm{d}\bar{x}}{\mathrm{d}s} = -\cos\bar{\gamma} \\ \frac{\mathrm{d}}{\mathrm{d}s}(\bar{T}\sin\bar{\gamma}) &= -\bar{Z} - \rho_c g, \qquad \frac{\mathrm{d}\bar{z}}{\mathrm{d}s} = \sin\bar{\gamma} \end{aligned} \tag{37}$$

The values of $\bar{T}_N$ and $\bar{\gamma}_N$ given by Eq. (36) are used as starting values, and the integration proceeds in a straightforward way in $-s$ from l to 0 (for this calculation, the origin needs to be moved to P_N). It is advisable to compute many more points than N on the cable in the steady state to ensure accurate values of the variables' derivatives at the N main points.

E. System Structure

We define the following vectors:

primary variables $(6N + 2)$

$$\begin{aligned} \boldsymbol{\xi} &= [\xi_1 \ldots \xi_N]^T, \qquad \boldsymbol{\zeta} = [\zeta_1 \ldots \zeta_N]^T \\ \boldsymbol{u} &= [u_1 \ldots u_{N-1}]^T, \qquad \boldsymbol{w} = [w_1 \ldots w_{N-1}]^T \\ \boldsymbol{h}' &= [h_1' \ldots h_N']^T, \qquad \boldsymbol{T}' = [\,T_1' \ldots T_N']^T \\ \boldsymbol{b} &= [u'w'q'\theta']^T \end{aligned} \tag{38}$$

The foregoing are assembled into

$$\boldsymbol{x}_1 = [\boldsymbol{\xi}\ \boldsymbol{\zeta}\ \boldsymbol{u}\ \boldsymbol{w}\ \boldsymbol{h}'\ \boldsymbol{T}'\ \boldsymbol{b}]^T \tag{39}$$

auxiliary variables $(4N + 2)$

$$\begin{aligned} \boldsymbol{y} &= [u_N - w_N]^T, \qquad \boldsymbol{X}' = [X_1' \ldots X_N']^T \\ \boldsymbol{Z}' &= [Z_1' \ldots Z_N']^T, \qquad \boldsymbol{\gamma}' = [\gamma_1 \ldots \gamma_N']^T \\ \frac{\mathrm{d}}{\mathrm{d}s}\boldsymbol{\gamma}' &= \left[\frac{\mathrm{d}}{\mathrm{d}s}\gamma_1' \ldots \frac{\mathrm{d}}{\mathrm{d}s}\gamma_N'\right]^T \end{aligned} \tag{40}$$

which are assembled into

$$\boldsymbol{x}_2 = \left[\boldsymbol{X}'\ \boldsymbol{Z}'\ \boldsymbol{\gamma}'\ \frac{\mathrm{d}}{\mathrm{d}s}\boldsymbol{\gamma}'\right] \tag{41}$$

By virtue of Eqs. (14), (21), and (24), we can express x_2 as a function of x_1

$$\boldsymbol{x}_2 = \boldsymbol{Q}_4\boldsymbol{x}_1 \tag{42}$$

In terms of the preceding variables, we can rewrite the previously derived governing equations in convenient matrix form. For example, Eq. (7a) applied at the N points P_n becomes

$$\boldsymbol{I}\dot{\boldsymbol{\xi}} = \boldsymbol{I}\boldsymbol{u} + \boldsymbol{A}_1\boldsymbol{y}, \qquad \boldsymbol{I}\dot{\boldsymbol{\zeta}} = \boldsymbol{I}\boldsymbol{w} + \boldsymbol{B}_1\boldsymbol{y} \tag{43}$$

When treating Eqs. (7b) and (7c) we use a finite difference approximation to $\mathrm{d}T'/\mathrm{d}s$, i.e.,

$$\frac{\mathrm{d}T'}{\mathrm{d}s} = \frac{T'_{n+1} - T'_{n-1}}{2\bar{h}}$$

The result of applying Eqs. (7b) and (7c) at the $N - 1$ points, $P_1 \ldots P_{N-1}$ is then the $2N - 2$ equations

$$\begin{aligned} \rho_c\boldsymbol{I}\dot{\boldsymbol{u}} &= \boldsymbol{C}_1\boldsymbol{X}' + \boldsymbol{C}_2\boldsymbol{T}' + \boldsymbol{C}_3\boldsymbol{\gamma}' + \boldsymbol{C}_4\frac{\mathrm{d}}{\mathrm{d}s}\boldsymbol{\gamma}' \\ \rho_c\boldsymbol{I}\dot{\boldsymbol{w}} &= \boldsymbol{D}_1\boldsymbol{Z}' + \boldsymbol{D}_2\boldsymbol{T}' + \boldsymbol{D}_3\boldsymbol{\gamma}' + \boldsymbol{D}_4\frac{\mathrm{d}}{\mathrm{d}s}\boldsymbol{\gamma}' \end{aligned} \tag{44}$$

Equations (17) and (16) are similarly written as

$$c_2\boldsymbol{I}\dot{\boldsymbol{h}}' = \boldsymbol{E}_1\boldsymbol{h}' + \boldsymbol{E}_2\boldsymbol{T}' \tag{45a}$$

$$0\boldsymbol{I}\dot{\boldsymbol{T}}' = \boldsymbol{D}_1\boldsymbol{h}' + \boldsymbol{D}_2\boldsymbol{\xi} + \boldsymbol{D}_3\boldsymbol{\zeta} \tag{45b}$$

The somewhat unusual appearance of the zero on the left side of Eq. (45b) is an artifice to facilitate the inclusion of Eq. (16) in the system of differential equations and $\boldsymbol{T}'$ in the state vector. The alternative, which is undesirable, is to eliminate $\boldsymbol{T}$ from the system altogether. The differential equations (29) of the body are rewritten as

$$\boldsymbol{F}_1\dot{\boldsymbol{b}} = \boldsymbol{F}_2\boldsymbol{b} + \boldsymbol{F}_3\boldsymbol{T}' + \boldsymbol{F}_4\boldsymbol{\gamma}' \tag{46}$$

and finally, the match conditions [Eq. (34)] allow us to write

$$\boldsymbol{y} = \boldsymbol{Q}_5\boldsymbol{x}_1 \tag{47}$$

Equations (43–46) are now assembled into the single equation:

$$\boldsymbol{P}\dot{\boldsymbol{x}}_1 = \boldsymbol{Q}_1\boldsymbol{x}_1 + \boldsymbol{Q}_2\boldsymbol{x}_2 + \boldsymbol{Q}_3\boldsymbol{y}$$

which, by virtue of Eqs. (42) and (47), becomes

$$\boldsymbol{P}\dot{\boldsymbol{x}}_1 = (\boldsymbol{Q}_1 + \boldsymbol{Q}_2\boldsymbol{Q}_4 + \boldsymbol{Q}_3\boldsymbol{Q}_5)\boldsymbol{x}_1 \tag{48}$$

Equation (48) is the final result for the longitudinal case. It is the equation of a generalized eigenvalue problem, which is readily solved with available software. (The generalized case differs from the canonical case, in which $\boldsymbol{P} = \boldsymbol{I}$, in that $\boldsymbol{P}$ here is singular and has no inverse.)

IV. Lateral Model

In the model for infinitesimal lateral motion, all of the steady-state displacements are zero, and the displacement and velocity of the cable are in the y_I direction. The body variables are $[v' \; p \; r \; \phi \; \psi]$ (Ref. 7). (The prime on v is to distinguish it from the cable velocity.) As noted previously, the lateral motions occur independently of the longitudinal ones only for a symmetric vehicle and only for infinitesimal motions.

A. Cable

When the cable has a lateral displacement, the tangent vector $\boldsymbol{t}$ is

$$\boldsymbol{t} = \left[\frac{\partial x_I}{\partial s} \; \frac{\partial y_I}{\partial s} \; \frac{\partial z_I}{\partial s}\right]^T \tag{49}$$

Because $\bar{y} = 0$, then $y = \eta$ and the y_I component of $\partial/\partial s(\boldsymbol{t}T)$ is $\partial/\partial s[(\partial\eta/\mathrm{d}s)T]$. The cable equations of motion in the y_I direction are then [cf. Eqs. (5) and (6)]

$$\dot{\eta} = v, \qquad \rho_c \dot{v} = Y' + \frac{\partial \bar{T}}{\partial s}\frac{\partial \eta}{\partial s} + \bar{T}\frac{\partial^2 \eta}{\partial s} \tag{50}$$

The aerodynamic force is given by

$$Y' = \frac{\partial Y}{\partial v}v = -\left(\frac{\bar{D}}{V_0} + \frac{\bar{L}}{V_0 \tan\bar{\gamma}}\right)v \tag{51}$$

1. Length Condition

The cable segment length h_n satisfies the relation

$$(x_n - x_{n-1})^2 + (y_n - y_{n-1})^2 + (z_n - z_{n-1})^2 = h_n^2$$

By taking the time derivative of this equation and recalling that x and z are constants in a lateral disturbance, we get to first order

$$(\bar{y}_n - \bar{y}_{n-1})(\dot{\eta}_n - \dot{\eta}_{n-1}) = h_n \dot{h}_n \tag{52}$$

But $\bar{y}$ is zero, so the segment length is constant in lateral motion. It follows that the tension T is also constant in time.

2. Towed Body

The model for the body is, like the longitudinal one, derived from that for an airplane by adding the cable forces [Ref. 7, Eq. (4.9, 19)], with the aerodynamic and inertial coefficients of a bisymmetric configuration. The equations of motion are written for principal body axes and, because of symmetry, with Y_p, N_p, L_v, L_r all equal to zero.

The matrix equation is

$$\begin{bmatrix} \dot{v}' \\ \dot{p} \\ \dot{r} \\ \dot{\phi} \\ \dot{\psi} \end{bmatrix} = \begin{matrix} \frac{Y_v}{m} & (V_0 \sin\bar{\theta}) & \left(\frac{Y_r}{m} - V_0\cos\bar{\theta}\right) & g\cos\bar{\theta} & 0 \\ 0 & \frac{L_p}{I_x} & 0 & 0 & 0 \\ \frac{N_v}{I_z} & 0 & \frac{N_r}{I_z} & 0 & 0 \\ 0 & 1 & \tan\bar{\theta} & 0 & \\ 0 & 0 & \sec\bar{\theta} & 0 & \end{matrix} \times \begin{bmatrix} v' \\ p \\ r \\ \phi \\ \psi \end{bmatrix} + T_{Ny} \begin{matrix} \frac{1}{m} \\ \frac{b'}{I_x} \\ \frac{a}{I_z} \\ 0 \\ 0 \end{matrix} \tag{53}$$

Resolving T_N into the y_B direction, we get

$$T_{Ny} = \bar{T}_N\left(-\psi\cos\bar{\gamma}_N + \phi\sin\bar{\gamma}_N - \left.\frac{\partial\eta}{\partial s}\right|_N\right) \tag{54}$$

The condition that has to be satisfied at the attachment point is that the y_I component of cable velocity relative to atmosphere is the same as that of the body. The match conditions are then

$$\dot{\eta}_N = v_N, \qquad \dot{v}_N = \dot{v}' + V_0\dot{\psi} + \dot{r}a + \dot{p}b' \tag{55}$$

The foregoing equations are assembled into the system matrix equation, with state vector

$$\boldsymbol{x}_1 = [\eta_1 \ldots \eta_N | v_1 \ldots v_N | v' \; p \; r \; \phi \; \psi]^T \tag{56}$$

and auxiliary vector

$$\boldsymbol{x}_2 = [T_{Ny}] \tag{57}$$

The assembly is then similar to the longitudinal case, i.e.,

$$\boldsymbol{P}\dot{\boldsymbol{x}}_1 = \boldsymbol{Q}_1\boldsymbol{x}_1 + \boldsymbol{Q}_2\boldsymbol{x}_2, \qquad \boldsymbol{x}_2 = \boldsymbol{Q}_3\boldsymbol{x}_1 \tag{58}$$

$$\dot{\boldsymbol{x}}_1 = \boldsymbol{P}^{-1}(\boldsymbol{Q}_1 + \boldsymbol{Q}_2\boldsymbol{Q}_3)\boldsymbol{x}_1 \tag{59}$$

In constructing Eq. (58), we use Eq. (50) at points 1 to $(N - 1)$, Eq. (55) at point N, and Eq. (53) for the body. The result

Table 2 Reference periods[a]

Case	Formula	Values	Data
1. Simple pendulum	$2\pi\sqrt{l/g}$	10.99	$l = 30$ m
2. Mass on a spring (bounce mode)	$2\pi\sqrt{\delta/g}$	1.099	$\delta = 0.01l$
3. Transverse vibrations of a taut string	$2\frac{l}{n}\sqrt{\rho_c/T}$	$1.74/n$	$\rho_c = 0.25$ kg/m $T = 30$ g N
4. Longitudinal vibrations of an elastic string	$2\frac{l}{n}\sqrt{\mu/E}$	$0.012/n$	$\mu = 7.9 \times 10^3$ kg/m^3 $E = 2 \times 10^{11}$ N/m^2
5. Single degree of freedom in pitch (or yaw)	$2\pi\sqrt{I_y/M_\alpha}$	$20.57/V_0$	——

[a]Seconds.

is $(2N + 5)$ equations in $(2N + 5)$ unknowns. This time $\boldsymbol{P}$ is nonsingular and the system takes on the canonical form [Eq. (59)].

V. Computations

Eigenvalues and eigenvectors were calculated for some examples with Eqs. (48) and (59) using the EIG command of MATLAB (Mathworks, Inc., Natick, Massachusetts). For Eq. (59), which is the canonical case, no special comment is required. However, for Eq. (48), $\boldsymbol{P}$ and $\boldsymbol{Q} = (\boldsymbol{Q}_1 + \boldsymbol{Q}_2\boldsymbol{Q}_4 + \boldsymbol{Q}_3\boldsymbol{Q}_5)$ have dimensions $(6N + 2)$, and the software returns $(6N + 2)$ eigenvalues. But the number of independent variables and, hence, the rank of the matrices, is only $(4N + 2)$. Thus, $2N$ of the eigenvalues are spurious. These are easily recognized, as they will be designated either by NAN (not a number) or by an excessively large number such as 10^{16}. When $c_2 = 0$, the rank is further reduced by N, and there are only $(3N + 2)$ meaningful eigenvalues. For the example cases in the following text, in which all the modes are oscillatory, the mode of highest frequency always corresponds to the points P_n forming a sawtooth pattern. This is of course not physically realistic, and hence, a number of the highest-frequency modes are rejected as not being meaningful. The number of useful modes at the low-frequency end of the spectrum depends on the value of N. Because the focus of interest is the towed body and it experiences appreciable motion only in the lowest few modes, we found that useful results could be obtained with N as small as 7. In the calculations made for the following figures, and for the validation checks, we used various N up to 30.

Table 3 Lateral stability derivatives

	C_y	C_l	C_n
β	−11.8	0	36.2
p	0	−100	0
r	83.5	0	−423

The programs used were validated by applying them to several limiting cases for which exact solutions are known. One was the simple pendulum, a point mass on a massless string in a vacuum A second was the same with the point mass replaced by a finite rigid body. The third was a classical mass-spring system, the body oscillating vertically on the flexible cable, and the fourth was the dangling inextensible flexible cable with no mass attached, also in a vacuum.[8] The limiting cases were approximated by using the programs at very low flight speed, e.g., 0.1 m/s, and very small masses for the cable or the body, as the case might be (the programs as written did not tolerate zeros for speed or masses). The periods of oscillation calculated by the program were close enough to the exact solutions to provide entirely satisfactory validation.

A. Reference Frequencies

It is very useful to have a set of reference frequencies at hand to provide a frame of reference against which to evaluate the frequencies returned by the computation. Table 2 gives

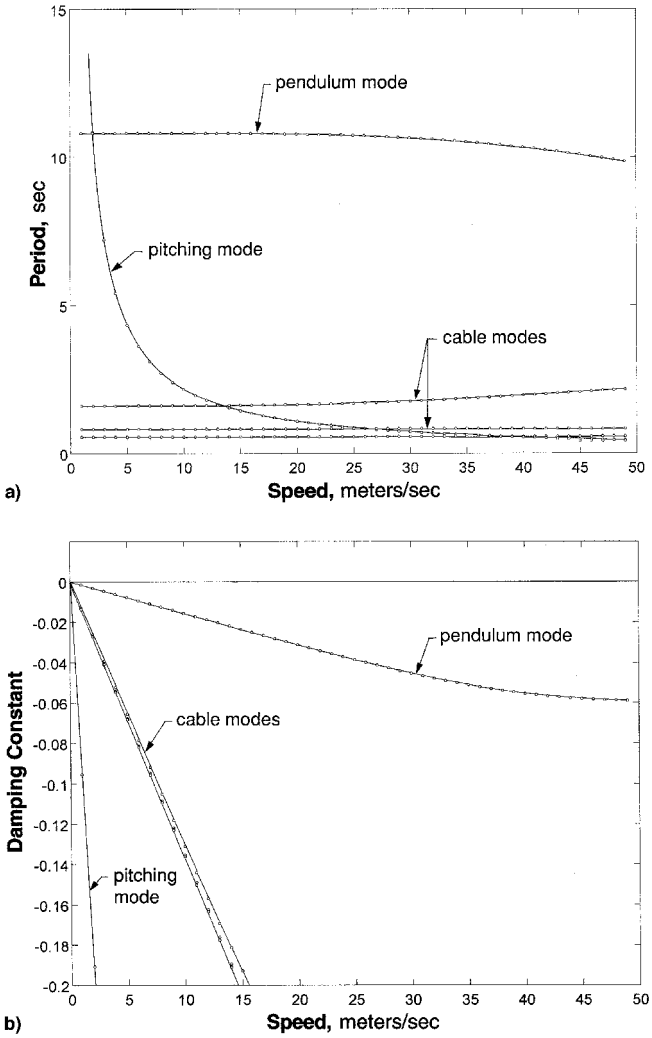

Fig. 4 Basic case: a) periods and b) damping of longitudinal modes (inextensible cable, $a = b = 0$).

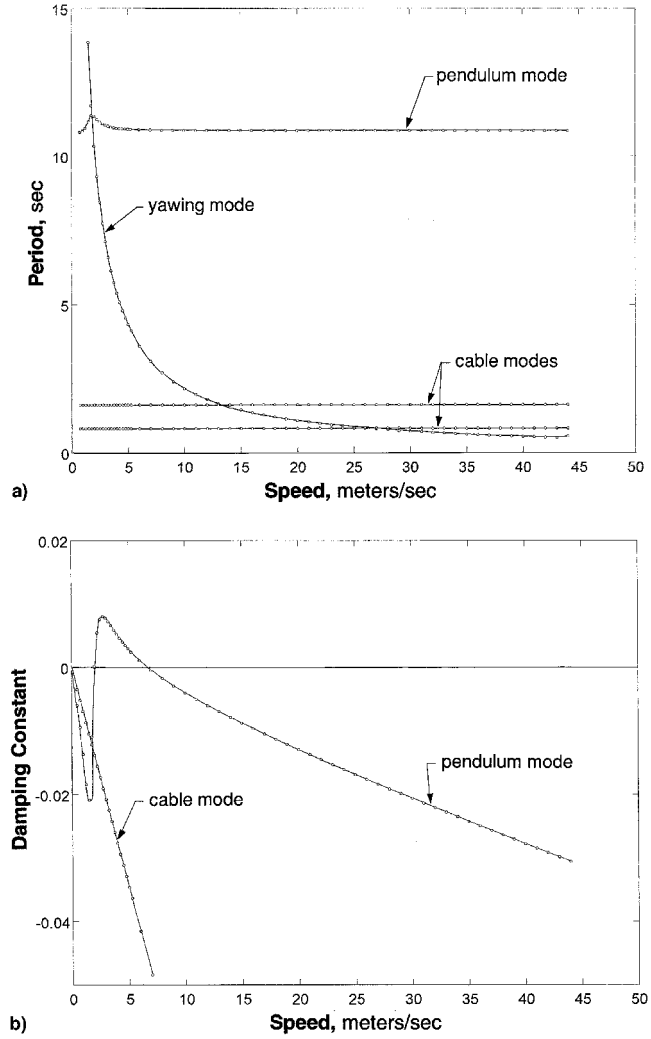

Fig. 5 Basic case: a) periodic and b) damping of lateral modes (inextensible cable, $a = b = 0$).

such a set, with the numerical values being those for the example cable and body used below. In Table 2, δ is the static deflection of the point P_N under the weight of the body; T is the tension in the cable, and μ and E are, respectively, its density and Young's modulus (values used are for steel); and n is the mode number.

The pendulum period stands out as the longest, except for the pitch degree of freedom at very low speed. It should be noted that the bounce mode corresponds to quasistatic extension of the cable, whereas item 4 corresponds to the propagation of elastic waves (sound waves) along the cable. The periods of the longitudinal waves are so short that they would not be expected to be of any interest except for extremely long cables. The principal effect of cable elasticity is thus expected to be related to the second item in the table, the vertical bounce of the body. The pitch (yaw) period goes from very large at low speed to very small at high speed. Thus, it crosses over some of the other periods at some speeds. This crossover turns out to be a cause of instability.

The example cable/body system has the following characteristics:

1) Attachment: the cable is attached to a fore and aft sling fastened to the top of the body in the xz plane (Figs. 1 and 3).

2) Cable: length 30 m; diameter 5 mm; and mass 0.25 kg/m.

3) Body: (reference area for coefficients is the body cross section) m_b = 30 kg; I_x = 0.3 kg m^2; I_y, Iz = 0.8 kg m^2; C_D = 0.3 + 0.095C_L^2; $Cl\alpha$ = 12.1; $C_{m\alpha}$ = −36.2; and C_{mq} = −423. Lateral stability derivatives are as in Table 3.

B. Results for Periods and Damping

The periods and damping of the modes of interest are shown for various cases in Figs. 4–6. The damping is shown as the real part n of the eigenvalue. Thus, the modes are stable when n is negative and unstable when positive. Only a few of the modes are shown — in the plots of period, those with the longest period, and in the plots of damping, those with the least damping.

Figures 4a and 4b show the longitudinal modes for the basic case, i.e., when the cable is inextensible and attached at the c.g. of the body, and Figs. 5a and 5b show the lateral results for the same case. The graphs of periods show that the pitch and yaw modes are proportional to V_0^{-1} and are approximated by item 5 in Table 2. The pendulum modes at about 11 s are also fairly approximated by item 1 in Table 2. The periods of the pendulum and pitch/yaw modes are equal at a flight speed of about 2 m/s. Some of the modes of shorter period can also be identified with and approximated by ones shown in the table. The longitudinal modes are all seen to be stable, but there is one unstable lateral mode. This can be identified with the interaction of the yawing degree of freedom with the pendulum degree of freedom at about 2 m/s, the speed at which their periods are the same. This is the same result as was obtained in Ref. 4. The physical cause is resonance. The yaw oscillation produces a periodic side force that drives the pendulum motion in resonance, with the phase relation such that energy is fed into the pendulum degree of freedom over a finite

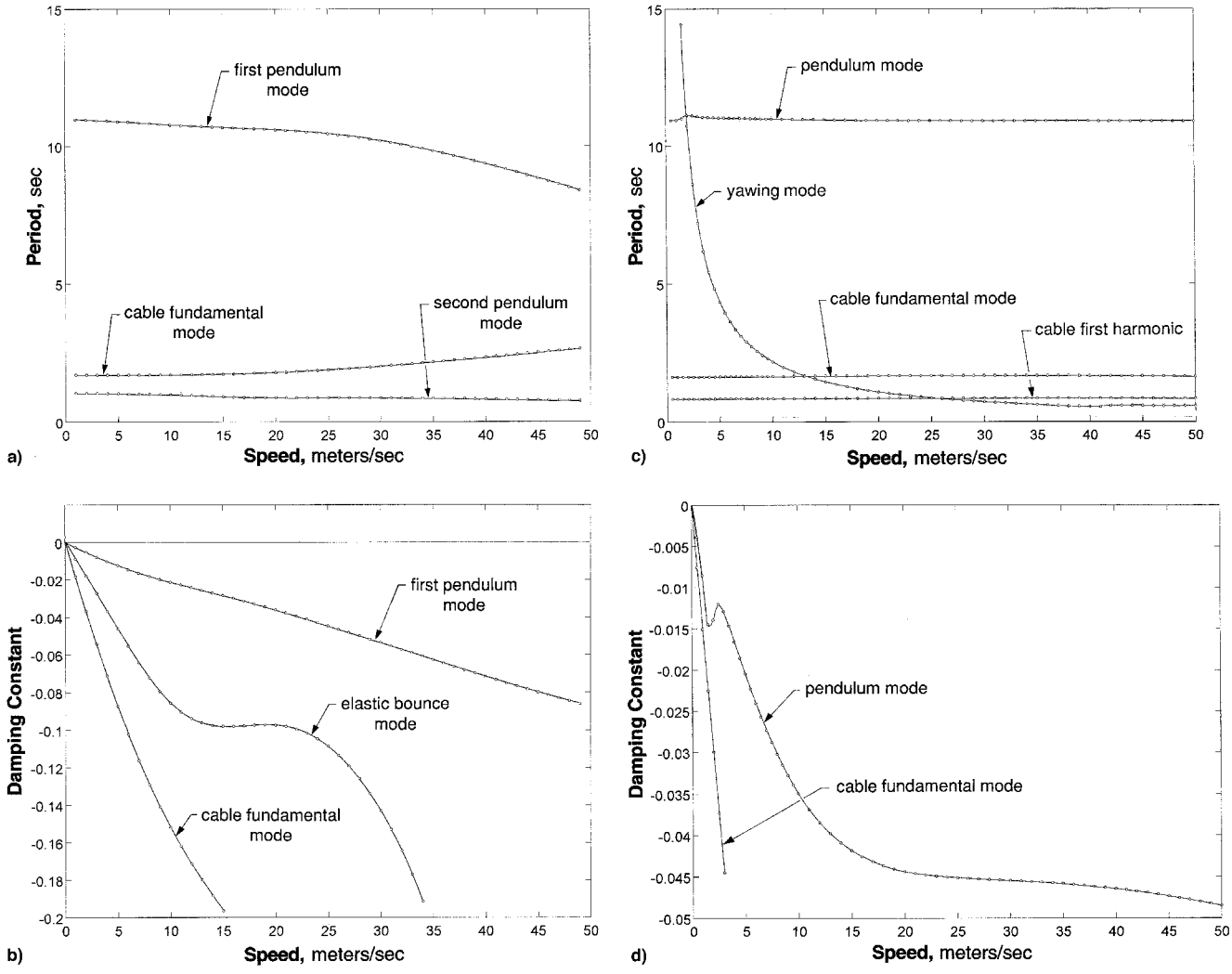

Fig. 6 Effect of elasticity and location of the attachment point: a) periods and b) damping of longitudinal modes (a = 0.2 m, b = 1.0 m, δ/l = 0.01). Effect of elasticity and location of the attachment point: c) periods and d) damping of lateral modes (a = 0.2 m, b = 1.0 m, b' = 0.18 m).

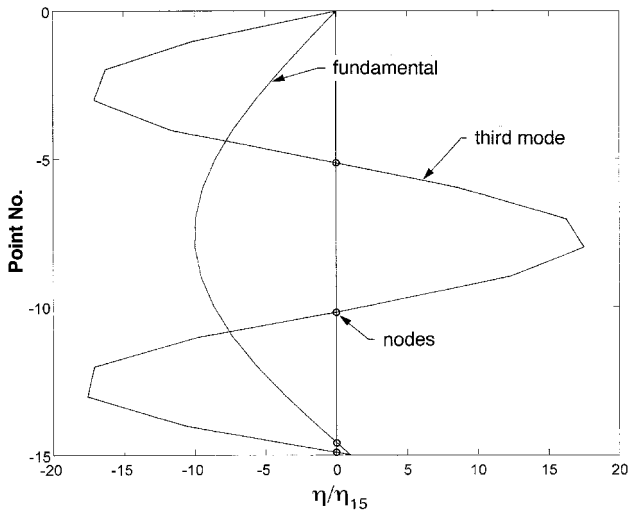

Fig. 7 Examples of shapes of cable modes (lateral) (N = 15, flight speed = 30 m/s, periods = 1.67 and 0.58 s).

range of forward speed. Although there is a similar crossover of frequency in the longitudinal modes, the pitch degree of freedom is only weakly coupled to the pendulum motion and does not produce a comparable instability. Pitch instability can occur with other values of the design parameters.

The addition of cable elasticity has relatively little effect on a short cable, such as that in the present example. With a long cable one would anticipate coupling of the vertical bounce and pitch degrees of freedom, with the potential for instability. This tendency is seen in Fig. 6b, which is for an elastic cable, at a speed of about 20 m/s.

The modal characteristics are profoundly altered by moving the attachment point of the cable off the c.g. The mode corresponding to item 5 of Table 2 disappears and is replaced by a pitch (or yaw) oscillation that is only slightly affected by flight speed. Moving the attachment point forward, by making a greater than zero, can eliminate the lateral instability. However, it is not practical to have a nonzero a without also having a nonzero b, otherwise the angle $\bar{\theta}$ would be too large (Fig. 3). A combination of a and b that yields both lateral and longitudinal stability with acceptable $\bar{\theta}$ is readily found by numerical experimentation. Figure 6 shows the results for a body hanging on an elastic cable.

C. Mode Shapes

The motion of the body in the lateral modes consists essentially of sideways swinging combined with yawing. There is very little rolling motion. Appreciable body motion is present only in the modes of lowest frequency. Higher-frequency modes consist mainly of sideways swinging of the cable from its steady-state position, the body c.g. being almost stationary. Figure 7 shows two of the lowest lateral modes, computed with 15 cable points, corresponding to the fundamental and third modes of a taut string, as in item 3 of Table 2. η_{15} is the displacement of the attachment point. Here, the bottom of the cable is not fixed, however, but is seen to have some motion, resulting in the presence of one node near the bottom. In the extreme, the mode of highest frequency has a sawtooth shape in which alternate points are of opposite sign. Clearly this latter shape is only crudely representative of a true sinuous shape. It is interesting, however, that the frequencies and damping obtained are more accurate than might be supposed from viewing the mode shapes.

In the longitudinal case, the motion of the body consists of an elliptical spiral trajectory of the c.g. in the vertical plane, combined with pitching. The cable motions are much like those shown for the lateral case.

VI. Conclusions

A computationally efficient mathematical model has been developed for the stability of flight-dynamic systems comprising two bodies joined by a flexible, elastic cable having internal damping. The model was applied to the case of a pendant heavier-than-air rigid finned body being towed beneath an aircraft on a short cable at constant speed. There is a range of speeds within which the system is unstable laterally if the cable is attached at the c.g. of the body. There is no comparable longitudinal instability in the example case. The lateral instability is an inherent property of bodies with fins that have weathercock static stability. The elasticity of the cable is not important for short cables but might be for long flexible cables. The lateral instability can be eliminated by attaching the cable forward of and above the c.g. of the body. This also reduces the potentially destabilizing effect of the elasticity of the cable.

Acknowledgments

Financial support was received for a related prior study that was the basis of much of this paper from High-Sense Geophysics, Toronto, Canada. The valuable contributions of my colleague J. H. De Leeuw are gratefully acknowledged. He provided many helpful discussions and valuable suggestions during the course of this work. Bruce Woodcock did much of the computer programming used to get results.

References

[1]DeLaurier, J. D., "A Stability Analysis for Tethered Aerodynamically Shaped Balloons," *Journal of Aircraft*, Vol. 9, No. 9, 1972, pp. 646–651.

[2]Bairstow, L., Relf, E. F., and Jones, R., "The Stability of Kite Balloons: Mathematical Investigation," Aeronautical Research Council, RM 208, UK, Dec. 1915.

[3]Glauert, H., "The Stability of a Body Towed by a Light Wire," Aeronautical Research Council, RM 1312, UK, 1930.

[4]De Matteis, G., "Dynamics of a Towed Sailplane," AIAA Paper 91-2862, Aug. 1991.

[5]Etkin, B., and Mackworth, J. C., "Aerodynamic Instability of Non-Lifting Bodies Towed Beneath an Aircraft," Univ. of Toronto, UTIA TR 65, Toronto, ON, Canada, 1963.

[6]Hoerner, S. F., *Fluid Dynamic Drag*, Hoerner, Midland Park, NJ, 1965, pp. 3–11.

[7]Etkin, B., and Reid, L. D., *Dynamics of Flight*, 3rd ed., Wiley, New York, 1995.

[8]Webster, A. G., *Partial Differential Equations of Mathematical Physics*, Dover, New York, 1966.